

Book of Tutorials and Abstracts



European Microbeam Analysis Society

EMAS 2011

**12th
EUROPEAN WORKSHOP**

on

MODERN DEVELOPMENTS AND APPLICATIONS IN MICROBEAM ANALYSIS

15 to 19 May 2011
at the
Centre de Congrès d'Angers
Angers, France

Organised in collaboration with
GN-MEBA - Groupement National de Microscopie
Électronique à Balayage et de microAnalyses



MULTI-SCALE RAMAN MICROANALYSIS OF ILL-ORGANIZED SOLIDS, AT THE LABORATORY OR WITH PORTABLE INSTRUMENTS

Philippe Colomban

Université Pierre-et-Marie-Curie (UPMC), CNRS, UMR7075, LADIR - Laboratoire de Dynamique, Interaction et Réactivité
2, rue Henry-Dunant, FR-94320 Thiais, France
e-mail: philippe.colomban@glvt-cnrs.fr

Philippe Colomban, born in 1952, was trained as a ceramic engineer (ENSCI- Sèvres). He started his research career in an industrial laboratory at Thomson-CSF (now THALES) where he prepared PLZT optically clear ceramics by sol-gel routes.

Then he moved to a CNRS in 1976, where he studied superionic and proton conduction. He became an expert in the synthesis of single crystals and sol-gel processed ceramics and glasses. In 1980 he created the Solid State Chemistry Group at the Ecole Polytechnique, Palaiseau. Simultaneously he works as consultant for the French Science and Technology Minister.

From 1989 to 1993 he was in charge of the new projects at the Materials Department of ONERA, the French Establishment for Aerospace Research and Development (sol-gel routes, oxide-oxide ceramic-matrix composites, microwave absorbing materials, and functionally graded composites, ...) and worked as consultant for them for 10 further years.

From 1994 to the present, as CNRS Fellow (1st classe Directeur de Recherche), his research interests include materials science and Raman, IR and neutron spectroscopies: stress and phase distribution imaging in composites, in situ analysis of solid state devices, fuel cells/electrolyser materials, synthetic and natural fibres, Attention is paid to the correlation between Raman parameters and mechanical and electrical (ionic, electronic) properties, as well to the identification of the technology used in ancient ceramics, glasses and pigments.

Philippe Colomban has been an invited speaker at international conferences in many different topics. His publications comprise more than 300 original papers and reviews or book chapters, and five patents. He is a member of the board of many Journals and Associate Editor of the Journal of Raman Spectroscopy.

1. ABSTRACT

Since a decade, a considerable number of instrumental developments have been made with regards to Raman microspectrometry (compact robust laser sources, new filters and architecture, increase of the PC capacity) leading to a variety of low cost and high sensitivity instruments to be used in many fields and coupled with other techniques. After a rapid presentation of the Raman spectroscopy, a combined analysis of the atom mechanics and charge transfer, its unique potential for the study of ill-organized covalent-bonded matter (glass, nano-materials, polymers, ...) will be illustrated. The Raman spectrometry combines a bottom approach of the nanoscale and a sub-micrometre optical resolution, well suited to build smart images by extracting judicious parameters from the spectra recorded by automatic mapping. We select examples chosen in the study of both advanced (PA66, PET, PBO, SiC, ...) and natural (silk, hair) proteic fibres, nano-sized compounds (CeO₂, ZrO₂, SiC, CdS, ...) as well as the analysis of cultural heritage master pieces (rock art, pastels and miniatures, pottery, glass, enamels,...) for identification and conservation purpose.

2. BRIEF HISTORY

The matter is made of atoms interacting with (iono)covalent, ionic or metallic bonds. The collective atom/molecule oscillations induce dipoles that interact with light. The penetration of light in a metal is limited to the very surface; consequently optical spectroscopies are generally used to analyze non-metal compounds. Infrared (IR) and near-IR (nIR) spectroscopies are widely used since decades. Attenuated total reflectance (ATR) microtechniques have simplified the spectrum collection; very limited or sometimes no preparation is now sufficient to analyze "soft" materials; the development of chemometric methods have drastically increased the efficiency, especially for poor quality spectra. However, the optical technique which developed the most rapidly since a few years is Raman scattering. Predicted theoretically in the beginning of the 20th century, experimentally demonstrated in 1928 by different groups in Russia, France and India (the Raman's group) [1] the technique has been used since the 70s due to the availability of powerful UV to visible range Ar⁺- or Kr⁺-ion lasers. The poor sensitivity of photomultiplier detectors requires high powers of illumination, a few hundreds of mW, typically. Consequently, only non-absorbent optically clear materials, mostly crystals may be analyzed. The time to record a spectrum ranges between 2 and 10 hours, as a function of the resolution! Since the 80s, high sensitivity photodiode arrays in combination with multichannel architecture have made it possible to decrease the illumination power at the sample to a few mW, and hence to study coloured samples. Subsequently, the development accelerates with the charge coupled device (CCD) matrix detection increasing the sensitivity drastically. The replacement of the first gratings stage used to reject the Rayleigh elastic scattering by a notch (a photonic "crystal") or edge (a set of dielectric layers) filter allows the design of very compact instruments with a very high sensitivity but with a

significantly lowered cost [2]. Simultaneously the miniaturisation of solid state laser sources and the increasing capacity of PC and laptop lead to a variety of spectrometers, from hand-detection to mobile or high-resolution fixed instruments excited with laser sources lined from UV to nIR [2]. Spectra are second-to-minutes recorded on a variety of samples, from colourless to black ones. The heating and associated phase transformations were a handicap to analyse heavy coloured samples and/or to use high magnification objectives (up to x200 objective i.e., x 2000 magnification) for long times. Recently, a Raman signature may be obtained for almost all type of iono-covalent bonded compound (Fig. 1) [3, 4]. The deposit of silver or gold metal nano-particles on the sample surface gives rise to surface enhancement Raman scattering (SERS) that makes possible the detection of molecule traces [5]. The latest trend in Raman spectroscopy is "hyper-spectral" imaging, where a computerized Raman mapping of a surface is used to image a physical or chemical property, after due processing of the spectral features [6, 7]. All these reasons motivate many groups to have a Raman instrument. However, there are a lot of tricky traps in the recording and interpretation of Raman spectra. We will address some of them and the potential of the technique regarding advanced nano-sized materials (polymers/proteic fibres, semi- and ionic conductor nano-materials) and cultural heritage artefacts (rock art, stained glass window and glass masterpieces, glazed pottery and enamelled metal).

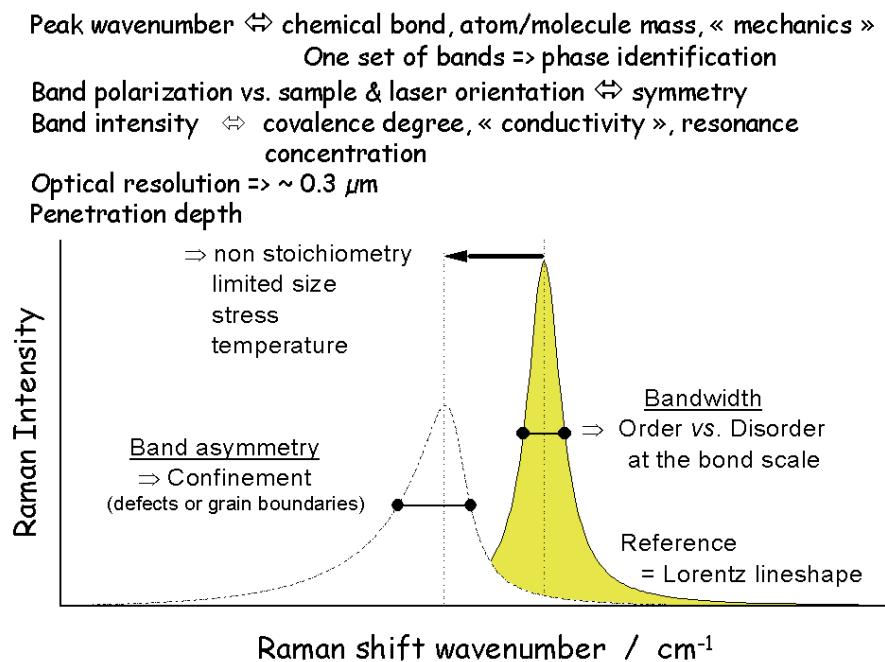


Figure 1. The basics of Raman spectra interpretation. The vibrational wavenumbers are often called Raman shifts as they correspond to a Raman-induced wavenumber shift of the scattered photons with respect to the laser excitation.

3. THEORY AND MODELS

The polarisation of a sample illuminated with light (electric field \vec{E}_0 ; frequency ν_0) is related to the chemical bond through the polarisability second rank tensor $\vec{\alpha}$ which depends on matter vibrations (the oscillations of atoms and molecules around their equilibrium positions):

$$\vec{P} = \vec{\alpha} \times \vec{E}_0 \cos(2\pi\nu_1 t) \quad (1)$$

The polarisation can be expressed as a function of the atomic displacement (normal coordinates) using a Taylor approximation, thus predicting elastic "Rayleigh" scattering ($\nu = \nu_0$, the exciting laser wave number) and inelastic "Raman" ($\nu = \nu_0 \pm \nu_{\text{vib}}$) scattering by atomic vibrations. The latter occurs if vibrations change polarisability ($\partial\alpha_{ij}/\partial Q \neq 0$) only. Other terms correspond to hyper and higher orders Raman scattering [3, 4]. Raman spectroscopists normally refer to the vibrations by their wavenumbers $\bar{\nu} = \nu_{\text{vib}}/c$ (c the light speed, $\bar{\nu}$ in cm^{-1} unit) and the classical electromagnetic theory of oscillating dipoles predicts that Raman peaks should have a Lorentzian shape. In disordered, nano-sized or amorphous compounds, because of the large distribution of local conformations, the band shape has a Gaussian or more complicated shape.

The signal intensity is predicted with the following formula [4]:

$$I_{\text{Raman}} \propto I_{\text{laser}} \bar{\nu}_{\text{laser}}^4 \left| \vec{e}_0 \cdot \vec{\alpha} \cdot \vec{e}_s \right|^2 d\Omega \quad (2)$$

where \vec{e}_0 and \vec{e}_s are unit vectors indicating the laser polarisation and direction of observation, respectively, whereas $d\Omega$ represents the solid angle of light collection, at a maximum when using high magnification, high aperture microscope objectives. Note, the 4 exponent leads to a very poor intensity with IR excitation. As polarisability ($\vec{\alpha}$) changes drastically from one bond to another, the Raman intensity may not be used to measure the relative amounts of different phases without preliminary calibration. This limitation can sometimes be an advantage when some secondary crystalline phases like pigments nano/microcrystals or dye molecules can be detected in very small quantities [4, 8, 9]. From a general point of view, elements with high atomic numbers from the right side of the periodic table (covalent materials) are good Raman scatterers whereas ionic bonded structures and protonic species are difficult to analyse with Raman spectroscopy. If the laser excitation wavelength fits with the absorption range of the electronic band, the interaction of light with electronic levels is anymore virtual and the resonance Raman spectra are drastically modified: a small wavenumber shift occurs but huge peak intensity modifications take places [3, 5, 8-10]. The presence of metal nano-particles / -films establishing an electronic transfer with the substrate or neighbouring molecules gives also raise to resonance (SERS) increasing significantly the sensitivity. The resolution (R) depends on the laser wavelength (λ) and the objective aperture (NA)

$$R = \frac{0.61 \lambda}{NA} \quad (3)$$

and may reach the diffraction limit, for example ~ 200 nm with violet laser, the optimum for available optics and lasers. This resolution is very close to that obtained with near-field (TERS, etc. [3]) techniques but the latter techniques work for very limited compounds.

For resonance Raman condition, the penetration depth of the laser beam can be very small [4] and it is possible to analyse specifically the material skin [6] and differentiate between the core and surface of a sample (Fig. 2) [10].

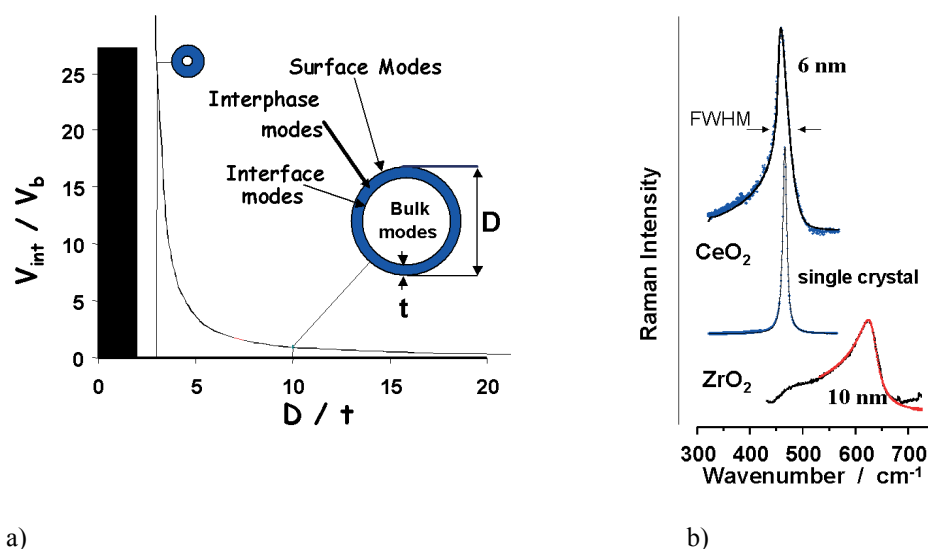


Figure 2. Discrimination between surface and bulk material: a) the interphase to bulk volume ratio in spherical nano-crystals with t outer interphase thickness; b) examples of grain size effect on ceria and yttrium-doped zirconia Raman spectra (after [4] and references herein).

4. "BLIND" DATA PROCESSING

In the (unfavourable but frequent) case when one has no preconceived idea about the Raman parameters most relevant to a specific issue, the comparison of spectra recorded on different samples and/or for different conditions is necessary. If nothing appears at first sight, a chemometric analysis (multivariate analysis: principal components analysis, factor analysis, ...; 2-dimensional correlation (C2D) [11-13]) might be very useful.

5. INSTRUMENTS AND PROCEDURES

Fig. 3 shows examples of the Raman technique versatility. Mobile laser and spectrometer, optic fibre connected to a remote optical head, allow the measurement out-side of the laboratory [14, 15]. The combination with a long working distance objective makes possible to couple the technique to other ones, directly (e.g., a universal tensile tester [16], Fig. 3b) or through a transparent window (diamond anvil cell [17], autoclave [18], kilns, through a translucent matrix [3], etc.).



Figure 3. Examples of the versatility of Raman microspectrometry: a) use of mobile Raman spectrometer and laser source to study rock art in Draggensberg National Park (South Africa; Photograph A. Tournié) [15]; b) the laser beam is focussed on a single silk fibre under controlled axial tension and soaked in water (Photograph P. Colombari) [13, 16].

6. DISORDERED MATERIALS

Due to its very local probe, the chemical bond polarisability, Raman scattering is very useful to study the structure of glass, amorphous or disordered compounds. Fig. 4 shows the example of SiC (with carbon traces) [19, 20] and CdS [21], both covalent bonded compounds made of layers that are subject to a 1D stacking disorder. This gives rise to a variety of phases (polytypes) and to very specific Raman signatures for each type of short range disorder, typically for coherence length ranging between 1 and 20 nm (Figs. 2 and 4). The electron-rich bonds generate a strong Raman scattering of their neighbouring species; this is well established for molecules (SERS) [5] but also for solid [22, 23].

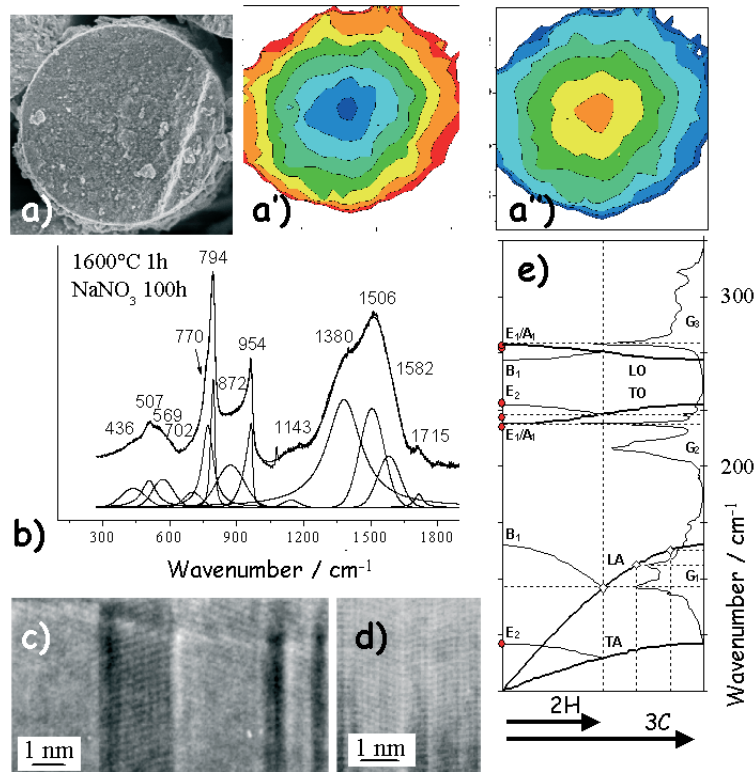


Figure 4. a) SiC fibre section ($d \sim 15 \mu\text{m}$), a') thermally treated SiC section Raman mapping of the sp^3 band wavenumber (1332 to 1345 cm^{-1} , green laser) and a'') smart image giving the fibre strength deduced from the relationship previously established [6]; b) Raman spectrum of the SiC fibre showing the different components: cubic nanocrystal ($794/954 \text{ cm}^{-1}$ LO/TO doublet), polytypic (770 cm^{-1}), amorphous and disordered SiC (optic bands + 400 - 700 acoustic and 870 cm^{-1} activated by the high disorder) and carbon traces (1140 - 1715 cm^{-1}); c and d), representative transmission electronic microscopy images: the stacking disorder and polytypes are obvious (courtesy L. Mazerolles, ICMPE Thiais) [19, 20]; e) off-resonance Raman spectrum (red exciting laser line) of a CdS crystal; as for SiC the acoustic ($< 180 \text{ cm}^{-1}$) and optic ($> 180 \text{ cm}^{-1}$) signatures of disordered polytypic (wurtzite 2H, ...) CdS layers superimpose to the TO/LO (~ 250 - 300 cm^{-1}) narrow doublet of 3C blend structure; the later doublet are solely present under resonance excitation (green laser); on the left, the phonon dispersion of acoustic and optic modes within the Brillouin zone is sketched [21].

Fig. 5 compares the Raman spectra of a Cu-containing glass [22]; the studied glass mimics the red glass layer used since the Middle-age for stained glass and since Celtic times for glass artefacts [24]. When the copper is reduced to form metal particles, the Raman scattering excited with a wavelength close to the Plasmon energy probes the environment of the particle only, not the matrix.

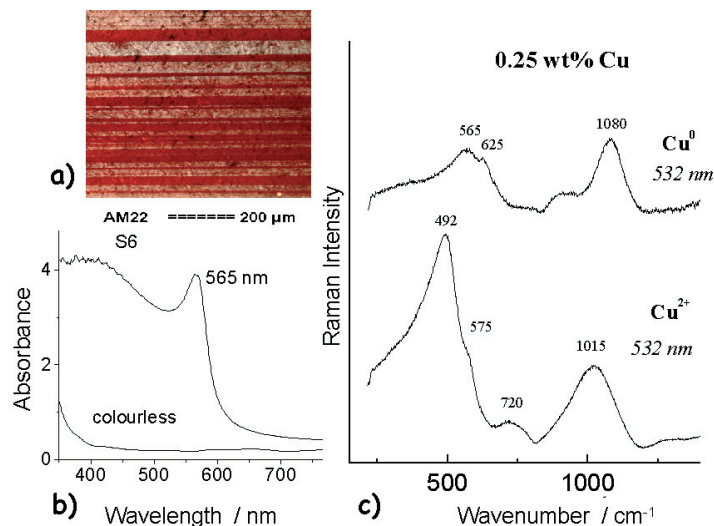


Figure 5. a) section of a flashed red stained glass alternating transparent and red layers, free or with copper (Cu^0) nanoparticles; b) UV-Vis absorption of Cu^0 -free and Cu^0 -containing glass, note the Plasmon resonance peak; c) comparison between the Raman signatures recorded with green excitation on the same 0.25 wt% Cu containing glass in form of Cu^{2+} -ions or as Cu^0 nano-particle [22].

7. MICRO- TO NANO-MECHANICS

Fig. 6 compares the Raman spectra of a polyethyleneterephthalate (PET) fibre at different degree of stretching: the precursor fibre as produced, after some hand stretching (x 5) and the commercial grade. The increase in crystallinity is evidenced by the narrowing of the lattice modes detected at ~ 70 and 110 cm^{-1} [16]. The stronger polarisation effect results from the alignment of the macromolecules along the fibre axis. These lattice modes are very useful to study the mechanical behaviour of the ultimate brick of the solid, the chemical bond.

For instance, the Raman shift across the diameter of a fibre (a PA66 polyamide in Fig. 7), both for the narrow (C : crystalline chains, Fig. 6a) and broad (α : amorphous chains) bands of the polymer gives information on the residual stress [16]. The compressive state of the amorphous phase in the fibre skin contributes to the highest mechanical properties. This anisotropic behaviour disappears after annealing above the glass transition temperature (T_g , Fig. 7a). Some other modes, the Amide I or the ν N-H ones probe very well the modification of the structure. For instance, the progressive wavenumber shift of the ν N-H mode of a polyamide PA66 fibre (Fig. 7b) reveals the regular shortening of the interchain distance under hydrostatic pressure; at $\sim 4 \text{ GPa}$ because of the contact between adjacent chains, the Amide I mode shifts progressively with increasing pressure [17].

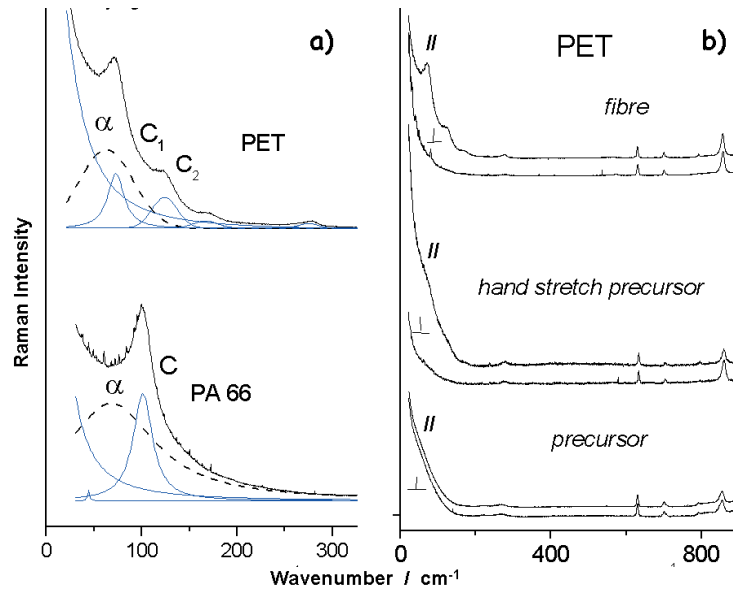


Figure 6. a) low wavenumber Raman “lattice” modes of PET and PA66 advanced fibres; the Lorentzian components arises from “crystalline” macromolecules and the Gaussian ones from amorphous ones; b) comparison between the polarized spectra recorded for a PET precursor, hand stretched and the commercial grade. Note the progressive increase of the macromolecule alignment (polarisation) and crystallinity (narrow peaks) [16].

Figs. 7 and 8 show the perfect agreement between the tensile macroscopic stress/strain behaviour of a fibre (synthetic PET or natural silk, the slope of the stress-strain curve at origin is the Young’s modulus) with the nano-mechanical behaviour of the amorphous phase for the exemplified PET fibre. In the PET fibre the nano-crystallites do not play a specific role: we observe a small up-shift due to the Poisson’ effect only.

The behaviour of silk fibres is highly variable but five different types can be recognized from the macroscopic tensile test [25]. The $\sim 2\%$ strain threshold is related to the lengthening of the helical fibroin macromolecules by untwisting, as observed also (but at 4 %) for keratin fibres. For instance, water incorporation in the silk (or keratin) fibre leads to Type II behaviour: the water lubricates the sliding of the macromolecule chains and hence the ultimate strain increases but the ultimate strength is decreased. The use of multivariate or 2D correlation technique is very useful when the spectra are studied as a function of one increasing parameter only [13]. For example, Fig. 7d shows the 2D plot of the spectra recorded for a keratin fibre submitted at increasing load up to the fracture. The specific behaviour of the signatures related to the chains belonging to helix or extended β sheet is obvious.

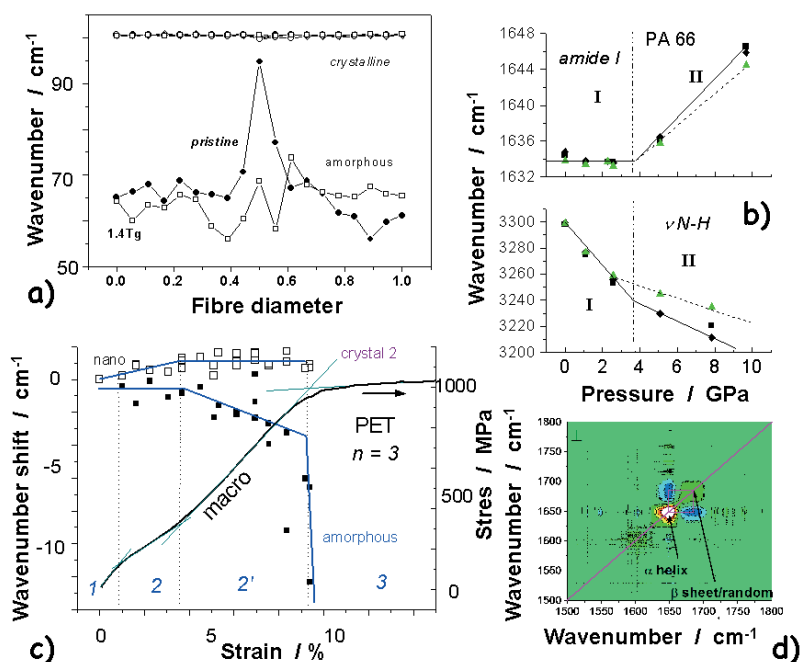


Figure 7. a) wavenumber plots across a PA66 fibre diameter measured before and after a thermal treatment at 1.4 Tg for the crystalline and amorphous “lattice” mode component (Fig. 6) [16];
 b) wavenumber plots as a function of the hydrostatic pressure for Amide I and ν N-H modes of a PA66 fibre [17];
 c) comparison of the Raman shift versus applied uniaxial tensile strain measured for the lattice mode wavenumber characteristic of the crystalline and amorphous PET macromolecules with the stress/strain curves;
 d) 2D correlation map calculated for hair single fibre under controlled strain [13].

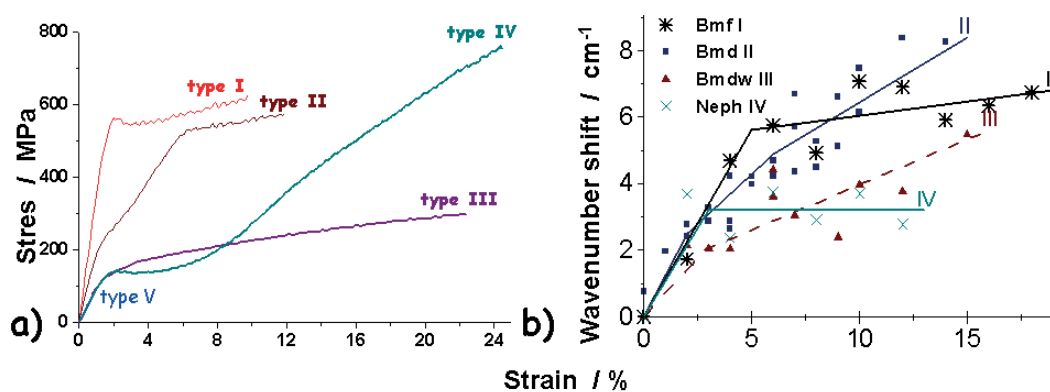


Figure 8. a) The five types of stress/strain macroscopic behaviour measured for silk fibres as a function of their history (I: very fresh, III: water saturated, IV: dried);
 b) the similar behaviour measured by their Raman shift at the chemical bond scale (using the $\sim 3300 \text{ cm}^{-1}$ ν N-H mode); the plateau corresponds to the lengthening of the helical fibroin macromolecules [25].

8. GLASS AND ENAMELS

The skill of potters and glass- or enamel-makers consists of a controlled modification of the three dimensional Si-O network by the replacement of Si^{4+} covalently bonded atoms by non-covalently (K^+ , Na^+ , Ca^{++} , Li^+ , ...) or poor-covalently bonded ones (Pb^{2+} , Ag^+ , ...). This decreases the number of Si-O bridges, and therefore softens the three-dimensional Si-O network what to control the melting/glazing temperatures and thermal expansion coefficient. The SiO_4 tetrahedron is a very strongly covalently-bonded chemical entity. It has a very characteristic vibrational spectrum signature, which is modified as a function of the connectivity of each SiO_4 tetrahedron versus its neighbours and because of the electric /"crystal field" perturbations due to neighbouring cations [26]. Since strong covalently bonded structures have Raman spectroscopic signatures orders of magnitude larger than those of ionic ones, the Raman spectrum of a silicate consists, as a first approximation, solely of the Si-O network signature (Si-O stretching, bending, and vibrational / collective modes, i.e., the so-called Boson peak) [3, 26]. Thus the Raman spectroscopic signature of crystalline and amorphous silicates depends on the silicate nano-structure, in particular on the different tetrahedron types (isolated (nesosilicate) or sharing 1 (sorosilicate), 2 (inno- and cyclosilicates), 3 or 4 (tectosilicates) oxygen atoms, Fig. 5c), and can be directly correlated to the glass composition (Fig. 9) as well as to its technology of production. For coloured, glazed and enamelled artefacts, the identification of the pigments is also a very efficient approach. Some pigments are used since millennia [25], but the palette has drastically since the 18th century for both inorganic and organic pigments, that gives good *post quem* chronological markers useful to establish restoration, embellishment or fakes [27-31]. The composition changes can be identified in a non-destructive way, with portable Raman instruments [26].

9. MOBILE INSTRUMENTS AND SENSORS

The robust lasers sources allow to work out of the laboratory, even in difficult conditions (Fig. 3). The first attempts have concerned the analysis of minerals with a strong, simple and easy recognisable Raman signature, i.e., the gemstone narrow peak signature in clean rooms. With the development of instruments and procedures – the poor resolution and complex baselines of mobile, compact spectrometers require specific procedures – more complex materials can be studied like ceramic and glass, even on building or on rock (see Table 1). In the same way dedicated sensors have been proposed [33]. A great development of mobile instruments (at/on line industrial control, forensic applications, ...) is expected in the very near future.

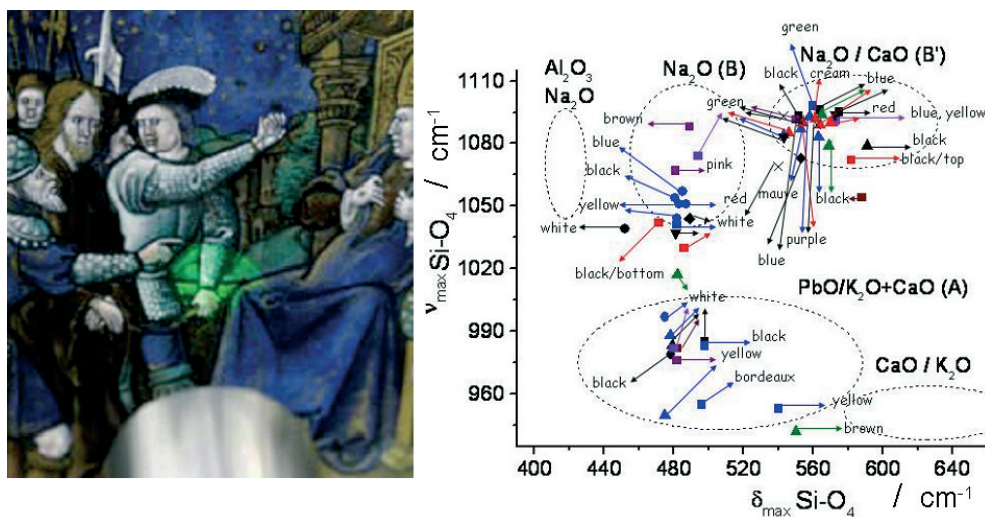


Figure 9. Limoges enamel (16th century, Musée des Arts décoratifs, Paris) analyzed at the museum with a mobile spectrometer; b) diagram of the SiO₄ stretching versus bending maximum (cm⁻¹) for series of Limoges enamels of various period of production; the dashed lines indicate the area of the main glass types (flux oxides are given).

Table 1. Measurements with portable Raman microspectrometers. A few examples.

Artefact	Materials	Laser nm	Place	Date	Ref.
Medici porcelain	Body, glaze & pigments	785	Sèvres Museum	2004	28
Iznik fritware	Body, glaze & pigments	532	Sèvres Museum	2004	29
Meissen porcelain	Body, glaze & pigments	532	Sèvres Museum	2006	30
windows	Stained glass	532	Sainte-Chapelle, Paris	2007	14
Cup, chalice, etc.	Enamelled glass	532	Sèvres Museum	2009	31
Rock art	Pigments	532	Mountain, South Africa	2010	15
Enamelled metal	Pigments & glass matrix	532	Paris Museum	2010	27
Vault paintings	Minerals	785	Antwerp Cathedral	2010	32

10. REFERENCES

- [1] Brillouin L (1922) *Ann. Physiq.* **17**: 88; Smekal A (1923) *Naturwissenschaften* **11**: 873; Raman C V and Krishnan K S (1928) *Nature* **121**: 501; Landsberg G and Mandelstram L (1928) *Naturwissenschaften* **16**: 557; Cabannes J (1928) *Compt. Rend. Acad. Sci.* **186**: 1201; Rocard Y (1928) *Compt. Rend. Acad. Sci.* **186**: 1107.
- [2] Bellot-Gurlet L and Colomban P (2010) *Ann. Falsifications Expert. Chim. & Toxic.* **973**: 45.

- [3] Gouadec G and Colomban P (2007) *Prog. Cryst. Growth Charact. Mater.* **53**: 1.
- [4] Nafie L (2001) in: *Handbook of Raman spectroscopy - From the research laboratory to the process line.* (Lewis I R and Edwards H G M, Eds.) Marcel Dekker Inc. (New York, NY): 1.
- [5] Schrader B (1995) in: *Infrared and Raman spectroscopy - Methods and applications.* (Schrader B, Ed.) VCH Verlag (Weinheim, Germany).
- [6] Colomban P (2003) *Spectroscopy Europe* **15**: 8.
- [7] Gouadec G, Bellot-Gurlet L, Baron D and Colomban P (2011) in: *Raman imaging.* (Zoubir A, Ed.) Springer Verlag.
- [8] Colomban P (2003) *J. Raman Spectrosc.* **34**: 420.
- [9] Faurel X, Vanderperre A and Colomban P (2003) *J. Raman Spectrosc.* **34**: 290.
- [10] El-Khalki A, Gruger A and Colomban P (2003) *Synth. Metals* **139**: 215.
- [11] Gouadec G, Forgerit J P and Colomban P (2002) *Comp. Sci. & Techn.* **62**: 505.
- [12] Widjaja E, Lim G H, Lim Q, Mashadi A B and Garlan M (2011) *J. Raman Spectrosc.* **42**: 2721.
- [13] Paquin R and Colomban P (2007) *J. Raman Spectrosc.* **38**: 504.
- [14] Colomban P and Tournié A (2007) *J. Cultural Heritage* **8**: 242.
- [15] Prinsloo L C, Tournié A, Paris C, Colomban P and Smith B (2011) *J. Raman Spectrosc.* **42**.
- [16] Colomban P, Herrera Ramirez J M, Paquin R, Marcellan A and Bunsell A (2006) *Eng. Fract. Mech.* **73**: 2463.
- [17] Colomban P, Sagon G, Lesage M and Herrera-Ramirez J M (2005) *Vib. Spectrosc.* **37**: 83.
- [18] Colomban P. and Slodczyk (2009) *Optical Mater.* **31**: 1759.
- [19] Havel M and Colomban P (2005) *Comp. Sci. & Techn.* **65**: 353.
- [20] Havel M, Baron D, Mazerolles L and Colomban P (2007) *Appl. Spectrosc.* **61**: 855.
- [21] Chi T T K, Gouadec G, Colomban P, Wang G, Mazerolles L, Thanh D X and Liem N Q (2011) *J. Raman Spectrosc.* **42**: 2793.
- [22] Colomban P and Schreiber H (2005) *J. Raman Spectrosc.* **36**: 884; Colomban P, Tournié A and Ricciardi P (2009) *J. Raman Spectrosc.* **40**: 1949.
- [23] Pham Thi M (1985) *Chem. Phys. Lett.* **115**: 130.
- [24] Colomban P (2009) *J. Nano Research* **8**: 109.
- [25] Jauzein V and Colomban P (2009) in: *Handbook of tensile properties of textile fibres.* (Bunsell A R, Ed.) Woodhead Publishing Ltd. / CRC Press (Oxford): 144.
- [26] Colomban P (2003) *J. Non-Cryst. Sol.* **323**: 180.
- [27] Kirmizi B, Colomban P and Blanc M (2010) *J. Raman Spectrosc.* **41**: 1240.
- [28] Colomban P, Milande V and Lucas H (2004) *J. Raman Spectrosc.* **35**: 68.
- [29] Colomban P, Milande V and Le Bihan L (2004) *J. Raman Spectrosc.* **35**: 527.
- [30] Colomban P and Milande V (2006) *J. Raman Spectrosc.* **37**: 606.
- [31] Ricciardi P, Colomban P, Tournié A and Milande V (2009) *J. Raman Spectrosc.* **40**: 604.

- [32] Deneckere A, Schudel W, Van Bos M, Wouters H, Bergmans A, Vandenabeele P and Moens L (2010) *Spectrochim. Acta A* **75**: 511.
- [33] Claverie R, Fontana M D, Durickovic I, Bourson P, Marchetti M and Chassot J M (2011) *Sensors* **10**: 3815.